

Internal Feedback in Biological Control: Diversity, Delays, and Standard Theory

Josefin Stenberg, Jing Shuang (Lisa) Li, Anish A. Sarma, John C. Doyle

Abstract—Neural architectures in organisms support efficient and robust control that is beyond the capability of engineered architectures. Unraveling the function of such architectures is challenging; their components are highly diverse and heterogeneous in their morphology, physiology, and biochemistry, and often obey severe speed-accuracy tradeoffs; they also contain many cryptic *internal feedback pathways* (IFPs). We claim that IFPs are crucial architectural features that strategically combine highly diverse components to give rise to optimal performance. We demonstrate this in a case study, and additionally describe how sensing and actuation delays in standard control (state feedback, full control, output feedback) give rise to independent and separable sources of IFPs. Our case study is an LQR problem with two types of sensors, one fast but sparse and one dense but slow. Controllers using only one type of sensor perform poorly, often failing even to stabilize; controllers using both types of sensors perform extremely well, demonstrating a strong *diversity-enabled sweet spot* (DESS). We demonstrate that IFPs are key in enabling this DESS, and additionally that with IFPs removed, controllers with delayed sensing perform poorly. The existence of strong DESS and IFP in this simple example suggest that these are fundamental architectural features in any complex system with diverse components, such as organisms and cyberphysical systems.

I. INTRODUCTION

Neural architectures and body plans have evolved to support exceptionally efficient and robust sensorimotor control, despite the fact that biological components communicate and compute more slowly and more noisily than engineered components. These differences and known neuroanatomy suggest that neural control architectures are unlike those currently found in engineering theory. Better understanding of neural architectures is beneficial for both neuroscientists and engineers, who wish to build systems that are as scalable, efficient, and robust as organisms, and with similarly constrained hardware.

A prominent feature of neural architectures that has eluded understanding is the presence of many *internal feedback pathways* (IFPs), whose role in biological control remains ambiguous. IFPs are prevalent in neuronal systems [3], [5]–[7] and can also be found in the immune system [8]–[10] and many others; for a more detailed survey of IFPs in biology, refer to our companion paper [1]. Survival-critical

J. Stenberg is with Engineering Physics, KTH Royal Institute of Technology. J. S. Li and J. C. Doyle are with Computing and Mathematical Sciences, California Institute of Technology. A. A. Sarma is with Computation and Neural Systems, California Institute of Technology. jossten@kth.se, {jsli, aasarma, doyle}@caltech.edu

This paper is one of three in a series on internal feedback in biological control architectures. These papers may be read in any order, though a suggested order is [1], then this, then [2].

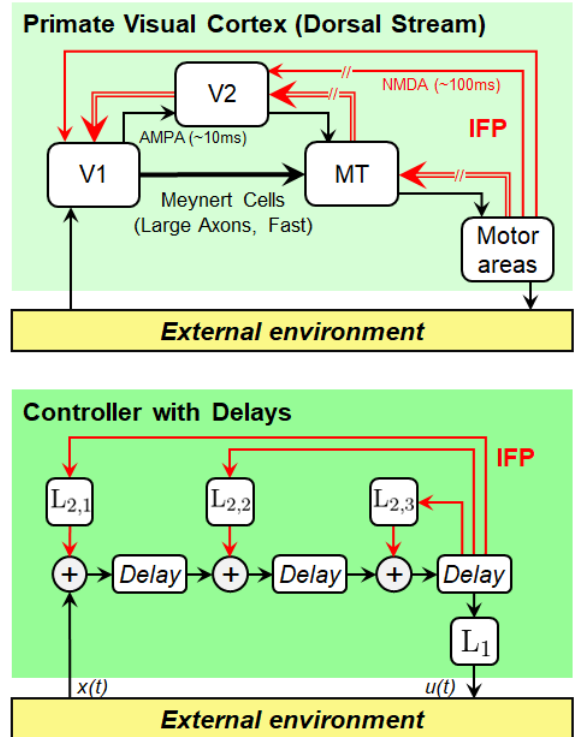


Fig. 1. Forward pathways are shown in black; internal feedback pathways (IFPs) are shown in red. The forward direction travels from sensing toward actuation (left to right); internal feedback travels from actuation back toward sensing (right to left). (Top) Primate visual cortex demonstrates existence of large amounts of IFPs [3]. Not shown are the diverse compositions of IFPs; each IFP arrow represents axon bundles with a range of sizes, receptors, and neurotransmitters corresponding to diverse speeds and accuracies. Fast forward pathways carry salient sensory information that gives rise to numerous internal feedback pathways, which influence processing in the forward path in a variety of ways. A theoretical framework is required to help guide and interpret future experiments, and clarify the function of IFPs. (Bottom) Controller with sensor delays and lots of IFPs, described in Sections III and IV. Delayed signaling is a central feature of the brain [4]; we wish to capture this feature in control-based models as well. The presence of delays in this controller motivates the presence of IFPs.

behaviors, such as reflexive escape and object-tracking, are typically thought to be generated by fast forward pathways, shown in black in the top panel of Fig. 1 for primate visual cortex. However, anatomical and physiological evidence tell us that the IFPs are more complex and diverse in speed and composition than forward paths, far more so than can be shown in a single figure. Such massive and diverse IFPs are a mystery since they have no obvious function for fast reflexes. Nonetheless, massive and diverse IFPs are found in almost all nervous systems across species and life stages. **We require**

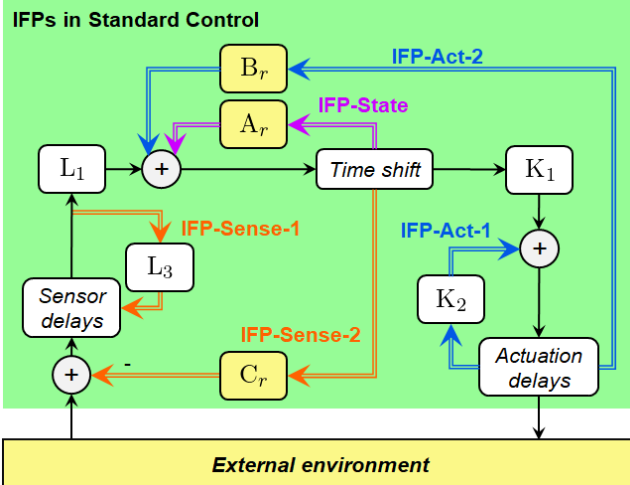


Fig. 2. IFP in output feedback (OF) controllers for a standard LQG problem. We include internal controller delays in sensing and actuation by augmenting the state with delays, and extending the standard separation theorem involving State Feedback (SF) and Full Control (FC). A , B , and C represent the state, actuation, and sensing matrices of the physical plant; K_1 , K_2 , L_1 , L_2 are submatrices of the optimal controller and observer gains. Delayed sensing and actuation induce two independent IFPs: IFP-Sense-1, and IFP-Act-1, which can be studied separately in the FC and SF subproblems. The remaining three IFPs (IFP-Sense-2, IFP-State, IFP-Act-2) are intrinsic to the Kalman filter in the OF controller.

new theory that explains the presence, complexity, and function of IFPs.

Another feature of neural architectures that remains somewhat mysterious is the vast diversity in morphology, physiology, and biochemistry of the underlying components. Due to energy constraints, these components often face *speed-accuracy tradeoffs* (SATs); they are either fast and inaccurate or slow and accurate but not both [4]. Recent work suggests that diverse hardware-level components (which obey SATs) and layered architectures enable performance that overcomes the hardware-level SATs [11]. For instance, organism behavior is both fast and accurate despite cells and neurons obeying SATs. We call this a *Diversity-Enabled Sweet Spot* (DESS).

We claim that IFPs are crucial architectural features that strategically combine highly diverse components to give rise to optimal performance; that they enable DESS. In this paper, we demonstrate this using a simple but striking model using slight modifications to existing control theory. We show that the presence of delayed sensing and/or actuation gives rise to new sources of IFPs in a standard output feedback controller, as shown by “IFP-Sense-1” and “IFP-Act-1” in Fig. 2. These IFPs are crucial for optimal performance, and can be studied separately in a full control problem with delayed sensing, or state feedback problem with delayed actuation. We set up a full control problem in Section II; this system combines accurate-but-delayed sensors and fast-but-inaccurate sensors. We then demonstrate the presence and importance of DESS (Section III) and IFPs (Section IV) in this system, and discuss the implications for general standard controllers. Concluding remarks are given in Section V.

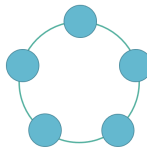


Fig. 3. The ring formation with $n = 5$ states where each state is connected to (and interacts with) two neighbors.

This paper focuses largely on the concepts of DESS and delay in requiring IFPs. We capture key elements of the problem using tools from standard control. We extend this work in our companion paper [2], where we utilize System Level Synthesis (SLS) [12] theory to show that incorporating additional features of biological systems (i.e. local and delayed communications) gives rise to optimal controllers containing a much greater complexity of IFPs. Unlike [13], we do not include new experimental data, but we aim to provide theory that assists in guiding and interpreting existing [14] and future experiments; we discuss potential experiments and biological systems of interest in our companion paper [1].

II. CASE STUDY

We now present the setup of a simple system with diverse sensing, in which we will analyze DESS (Section III) and IFP (Section IV). The goal of this analysis is not to model any particular biological system in fine detail, but to study simple, human-interpretable examples that give rise to fundamental theory on the existence and characteristics of DESS and IFP using standard control theory.

We consider a system of n nodes in a ring formation, as shown in Figure 3. State dynamics in this ring can be described by the difference equation $x_r(t+1) = A_r x_r(t)$, where $x_r \in \mathbb{R}^n$ represents ring states and $A_r \in \mathbb{R}^{n \times n}$ is:

$$A_r = \frac{a}{3} * \begin{bmatrix} 1 & 1 & 0 & \dots & 1 \\ 1 & 1 & 1 & 0 & \dots \\ 0 & \ddots & \ddots & \ddots & \vdots \\ \vdots & \ddots & \ddots & \ddots & 1 \\ 1 & 0 & \dots & 1 & 1 \end{bmatrix} \quad (1)$$

Here, the a parameter determines the spectral radius of A_r ; $a = 1$ corresponds to a neutrally stable system, and $a > 1$ corresponds to an unstable system.

We consider two types of sensors: fast and sparse, and slow and dense. This is reminiscent of biological components which obey speed-accuracy tradeoffs (e.g. proprioception vs. vision, retinal fovea vs. surround). These sensors lie on opposite ends of the speed-accuracy spectrum. We focus on the case of perfect actuation and diverse sensing, i.e. full control (FC), and assume zero sensor noise for simplicity¹. All analysis and findings naturally apply to the dual case of perfect sensing and diverse actuation, i.e. state feedback (SF). We will also briefly discuss the case of imperfect actuation

¹We assume zero sensor noise purely for pedagogical purposes; our findings on DESS and IFP are replicable with sensor noise, although the associated plots are slightly less cleanly interpretable.

and sensing in output feedback (OF) at the end of Section IV, and a simple extension to standard separation theory.

Consider the discrete-time linear time-invariant system

$$\begin{aligned} x(t+1) &= Ax(t) + B_2u(t) + B_1w(t) \\ y(t) &= Cx(t) \end{aligned} \quad (2)$$

where x , u , w , and y are the state, control action, disturbance, and output, respectively.

To model internal sensing delays, we add delay states to the model. Assume we sense each state, but with a delay of d timesteps; then, we introduce d copies of each ring state to represent information internal to the delayed sensors. The resulting state vector is $x = [x_r^\top \ x_s^\top]^\top \in \mathbb{R}^{n(d+1)}$. x_r corresponds to the original ring states; x_s represent delayed sensor states. Note: we define x_s as being internal to the agent; these correspond to the arrows exiting the delay blocks in Fig. 1. We can think of x_s as information sensed by the eye that is being passed along a delayed visual pathway to LGN, then V1, and so on. The motor areas of the brain can only access the most delayed information, i.e. the values of x_s corresponding to a delay of d ; these will be picked out by the ‘sensing’ matrix C .

For full control, we define the input vector $u = [u_r^\top \ u_s^\top]^\top \in \mathbb{R}^{n(d+1)}$; this has dimension equal to x . u_r represents physical actuation upon the ring states, and u_s denotes internal wires to internal delayed states; this corresponds to the red IFP arrows exiting the L blocks in Fig. 1. Although both u_r and u_s are control signals in the standard sense, they have vastly different interpretation and engineering cost; u_r represents physical actuation, which for an organism requires high-energy-cost muscle cells, etc, while u_s represents low-cost internal communication, i.e. neurons.

The state matrix A for the vector x including delay states has dimension $n(d+1) \times n(d+1)$, and can be written as

$$A = \begin{bmatrix} \hat{A}_r & 0_{n \times n} \\ I_{nd \times nd} & 0_{nd \times n} \end{bmatrix} \quad (3)$$

where $\hat{A}_r = [A_r \ 0_{n \times n(d-1)}]$ has dimension $n \times nd$, and I and 0 are identity and zero matrices of specified dimension. A has equal spectral radius as A_r ; its stability is also determined by a . For full control (FC), we have full actuation, i.e. $B_2 = I_{n(d+1) \times n(d+1)}$. Additionally, we only consider disturbances that affect the ring states, i.e. $B_1 = [I_{n \times n} \ 0_{n \times nd}]^\top$.

For fast and sparse sensing, instead of sensing each state, we choose to sense along eigenvectors of the ring state matrix A_r . We will choose some q eigenvectors, typically corresponding to the q highest-magnitude eigenvalues of A_r . C_f has dimension $q \times n(d+1)$, and is written as $C_f = [E \ 0_{q \times nd}]$, where the rows of $E \in \mathbb{R}^{q \times n}$ are the q selected eigenvectors of A_r . C_f represents instant sensing which senses along the q “worst directions” of impulse propagation. For slow and dense sensing, we sense each state with a delay of d timesteps. C_s is of size $n \times n(d+1)$, and can be written as $C_s = [0_{n \times nd} \ I_{n \times n}]$. We will study the

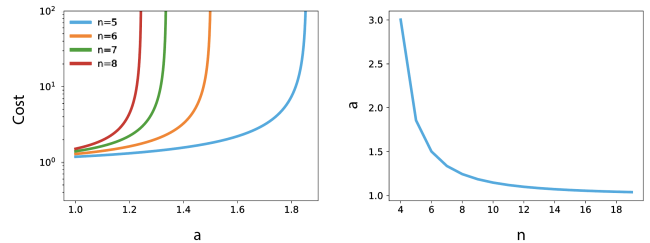


Fig. 4. System behavior with fast-only sensing. (Left) Cost as a function of stability a for different system sizes n . In all cases, the cost eventually diverges to infinity as the system becomes less stable and the controller fails to stabilize it. (Right) Maximum instability a that can be stabilized by the optimal controller, as a function of system size n . As system size grows, stabilization is increasingly challenging and we are only able to deal with systems with small instability.

system with fast-only, slow-only, and diverse (i.e. both fast and slow) sensors, corresponding to $C = C_f$, $C = C_s$, and $C = [C_f^\top \ C_s^\top]^\top$, respectively.

We consider a standard LQR cost with state penalty $Q = B_1 B_1^\top$. Note that we only penalize the n ring states, not the delayed sensing states. The optimal controller is $u(t) = -Ly(t)$, where $L = A^\top SC(C^\top FC)^{-1}$ for matrix S that solves the DARE. Assuming no sensor noise, the LQR cost can be calculated via $\text{Tr}(B_1^\top FB_1)^2$. We now use this system to demonstrate substantial presence of both DESS and IFPs.

III. DIVERSITY-ENABLED SWEET SPOT (DESS)

As described above, we consider two sensor types: fast and sparse, and slow and dense. We first study system performance with uniform sensors; this gives terrible performance and incurs extreme costs. We then use diverse sensors, which give a dramatic performance improvement and demonstrate the existence of a DESS. For the remainder of this paper, unless otherwise specified, we use parameters $n = 5$, $a = 1.856$ (to be explained), $q = 1$, and $d = 3$.

A. Fast-and-sparse sensing

For a controller with only fast-and-sparse sensing, we show the relationship between the cost and the stability value a in the left panel of Fig. 4. For each line, there is clearly a breaking point at which fast-only sensing results in instability and infinite cost. These breaking points occur when we reach a value of a that gives more than $q = 1$ unstable eigenvalues in A_r ; in this case, fast-only sensing is no longer sufficient for the controller to reject all directions of unstable impulse propagation. Thus, certain states never converge to zero, yielding infinite cost.

The right panel of Fig. 4 shows the breaking point values of a for which fast-only sensing results in infinite costs (i.e. fails to stabilize). As the system size n increases, the controller is less able to stabilize unstable open-loop systems. For large system sizes, the controller can only handle marginally unstable systems (i.e. a very close to 1).

²In plots, we will normalize the LQR cost by the number of ring nodes, i.e. cost = $\text{Tr}(B_1^\top FB_1)/n$.

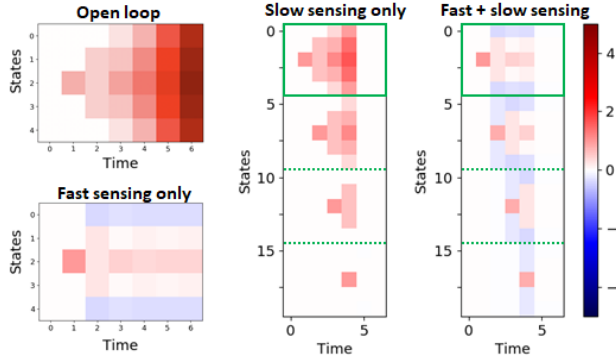


Fig. 5. Impulse responses for the ring system. For the center and right panels, the first 5 states (outlined in solid green) correspond to the true states on the ring, whereas later states represent internal, delayed sensor states corresponding to the ring states (separated by dotted green lines). (Left, Top) Open loop, cost = ∞ . The system is unstable and the states grow to infinity. (Left, Bottom) Fast-only, cost = ∞ . Notice that the state does not decay to zero. (Center) Slow-only, cost = 13.726. The impulse response propagates and amplifies until the delayed information about the impulse reaches the controller, at which point all states become zero. (Right) Diverse, cost = 2.279. The impulse response appears to be a mix of the fast-only and slow-only cases; some portion of the impulse is rejected right away, and all states become zero after delay d .

For $n = 5$, the minimum value of a that causes instability and incurs infinite cost is $a = 1.856$. The corresponding impulse response is shown on the left in Fig. 5. The impulse response does not get attenuated to zero, as expected.

B. Slow-and-dense sensing

Consider a controller with only slow-and-dense sensing: the impulse response is shown in the middle panel of Fig. 5. In the first three timesteps, the system behaves as if it were open-loop; no action is taken because due to delayed sensing, the controller does not yet know about the disturbance. Once the delayed information reaches the controller, the impulse propagation is immediately killed off, thanks to the dense information provided by the slow sensor.

C. Diverse sensing

Consider a controller with diverse sensors, i.e. both the fast-and-sparse and slow-and-dense sensors. The impulse response is shown in the right panel of Fig. 5. The diverse controller displays a mix of behaviors from the fast-only and slow-only setups. In the first three timesteps, the behavior is identical to the fast-only system; as soon as information from the slow sensor reaches the controller, all impulse propagation is completed attenuated and the state values go to zero. This controller also has much-improved cost; it incurs a performance cost that is nearly six times smaller than the best non-diverse setup. This displays a dramatic DESS.

We vary the delay parameter and show that this DESS only becomes more dramatic for increased values of delay; this is shown in Fig. 6. Clearly, the diversity in sensors achieves a sweet-spot; while fast-only sensing incurs effectively infinite costs and slow-only sensing incurs dramatic exponentially increasing costs, diverse sensing allows us to keep the cost below 10^1 . Thus, delayed sensing is acceptable if paired

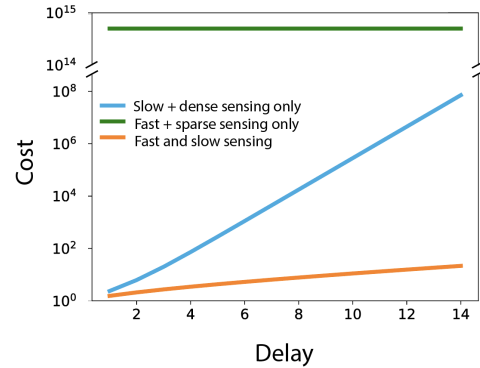


Fig. 6. Cost of controllers using fast-only, slow-only, and diverse (i.e. fast and slow) sensing for varying values of delay. The fast-only setup incurs effectively infinite cost across all values of delay. At low delay, the slow-only setup incurs cost on the same order of magnitude as the diverse setup. As delay is increased, the slow-only setup incurs dramatic, exponentially increasing costs, while the diverse setup maintains a low cost.

with a fast-but-sparse sensor; similarly, sparse sensing is acceptable if paired with dense-but-slow sensor. This sweet spot is consistent with what we expect from the sensorimotor system and neural systems in general; neurons and cells typically obey SATs, but a combination of diverse neurons (i.e. both fast and slow) allows the system to achieve a DESS.

Overall, this simple but striking example suggests that DESS is a fundamental feature in the presence of diverse components. Even with only two types of sensors, we observe a strong DESS. We expect that in systems with more diversity between components (i.e. biological and neural systems), even more extreme DESS may be found.

We remark that for systems with larger values of n and a , even more pronounced DESS is observed. This is because fast-only sensing becomes more sensitive to instability as n increases, as suggested in Fig. 4. On the other hand, increasing q improves the performance of the fast-only system. As long as q is less than the number of unstable eigenvalues in A_r , we observe dramatic DESS. When q is greater or equal to the number of unstable eigenvalues in A_r , we still observe a DESS, albeit less drastic one. Also, all analysis and results in this section apply to the dual case of diverse actuation, in which dramatic DESS is also observed.

Considering the terrible performance of the non-diverse setups, we conclude that the diverse setup of sensors performs far better than the sum of its individual parts. This illustrates a basic principle at work: by cleverly using architecture, we can combine individual components that together perform better than the sum of their parts (i.e. achieve a DESS). We now study a fundamental architectural feature that enables this DESS – internal feedback pathways (IFPs).

IV. INTERNAL FEEDBACK PATHWAYS (IFPs)

We now observe the structure of the controllers that give the dramatic DESS found above. We show that IFPs are an essential architectural feature that enable DESS and that removing IFPs destroys system performance.

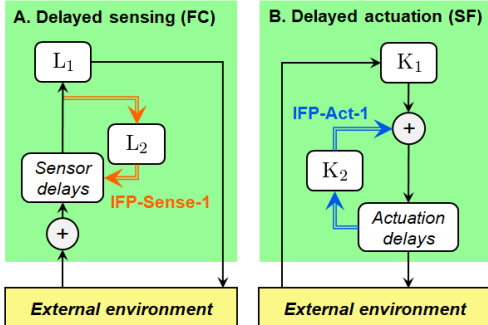


Fig. 7. Block diagrams displaying IFPs in standard controllers with delay. All forward processing is indicated by black arrows. (A) IFPs for the full control problem with delayed sensing is shown by the orange arrows. The optimal FC controller $L = [L_1^\top \ L_2^\top]^\top$ is partitioned into two parts representing forward processing and IFPs, respectively. For our controller, we can further partition L_2 into $L_2 = [L_{2,1}^\top \ L_{2,2}^\top \ L_{2,3}^\top]^\top$; a more detailed diagram is shown in the bottom panel of Fig. 1. (B) IFPs for the (dual) state feedback problem with delayed actuation is shown by the blue arrows. The optimal SF controller $K = [K_1 \ K_2]$ is partitioned into two parts representing forward processing and IFPs, respectively.

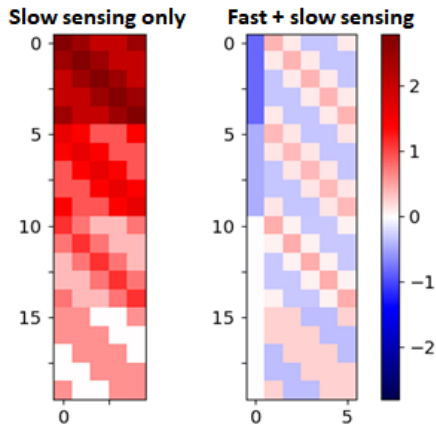


Fig. 8. The optimal controllers L for setups that include the slow sensor (and therefore IFPs). For both controllers, the first 5 rows correspond to forward paths, and the subsequent rows represent IFPs. In both controllers, IFPs are abundantly present. (Left) Controller with slow-only sensing. (Right) Controller with diverse (i.e. fast and slow) sensing.

We define IFPs in controllers as information traveling from the actuation output toward the sensor input of the controller. We show the presence of IFPs in our FC controller with delayed sensing and its dual (SF controller with delayed actuation) in Fig. 7. In our setup, our definition of the delay states as *internal, sensor states* means that all control action to them (i.e. the orange arrow exiting from L_2 in Fig. 7) constitute IFPs. This control action corresponds to internal wires in the controller rather than physical actuation upon the external environment. Conversely, in a system with no internal states, a static gain controller $u = Kx$ or $u = Ly$ would contain only forward paths from sensor input (x for SF and y for FC) to actuation output u , with no IFPs.

In our model, IFPs only appear in the model when the slow sensor (i.e. delayed internal states) is present, whether on its own or in a diverse-sensor setup. For the optimal FC

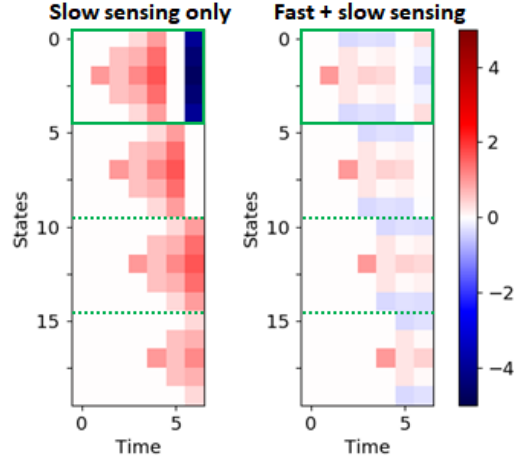


Fig. 9. Impulse responses of controllers with removed IFPs. Prior to removing IFPs, both controllers were able to stabilize the system. After removing IFPs, neither can. (Left) Slow-only sensing, cost = ∞ . (Right) Fast + slow sensing, cost = ∞ .

controller $L = [L_1^\top \ L_2^\top]^\top$ where $L_1 \in \mathbb{R}^{n \times n}$, entries in L_2 corresponds to IFP. We show our slow-only and diverse controllers from the previous section in Fig. 8. For the slow-only controller, the shape of the A_r matrix is clearly visible within both the forward and IFP blocks. This is not a coincidence, since both forward and feedback (i.e. IFP) paths utilize A_r to predict and counteract the behavior of the ring states. For the controller with both fast and slow sensors, the shape of the blocks are still similar, although including the fast sensor changes the magnitudes of the entries in the controller corresponding to the slow and dense sensor.

In both controllers, it is clear that the system uses IFPs to produce systems with optimal performance – in the case of the diverse controller, IFPs are required to give the DESS discussed in the previous section. To further study the impact of IFPs, we remove the IFPs in setups with slow and diverse sensing and observe the resulting performance. This is done by setting L_2 to be zero in the optimal controller.

A. System performance without IFPs

The removal of IFPs severely degrades performance, as shown in Fig. 9. *With* IFPs, both the slow-only and diverse controller delivered stable performance. After removing IFPs, both controllers become unstable.

Removal of IFPs causes a gap in system information about previously implemented actions and current state. The resulting system acts based on what has been sensed d time steps ago *without taking previous but more recent actions into account*. This is apparent in the impulse response of the slow-only setup on the left in Fig. 9. The impulse is attenuated perfectly after $d + 1$ time steps, when the controller has finally accessed the delayed sensed information. However, immediately in the next timestep, the states receive more attenuating control action, causing the zero states to become negative (due to the *positive* sensed state from d timesteps ago). Later, these negative states will be sensed, and positive control action will be taken. Zero-value states

will be achieved again, but additional attenuating control action (this time negative) will be taken, causing the zero states to become positive. The entire system will fluctuate between positive-value and negative-value states, each time growing in magnitude. Overall, the removal of IFPs causes the system with slow-only sensing to become unstable.

Removing IFPs in the diverse sensing case yields similarly bad results; the impulse response again fluctuates such that the amplitude increases to infinity. Compared to the slow-only setup, the initial state magnitudes are smaller; however, states eventually diverge due to instability.

An interesting observation: if we reduce the instability value a of the system, then a setup with fast-only sensing is sufficient to stabilize the system. If we add slow sensing to this to create a diverse sensing setup, then remove IFPs, the resulting system still fluctuates but eventually decays to zero instead of blowing up. In this case, the diverse setup is *worse* than the fast-only setup. This again emphasizes the importance of IFPs, not only for performance but also to facilitate DESS in systems where delays are present.

B. IFPs in Standard Controllers

In the above sections, we used standard full control (FC) models to describe a simplified model with sensing delays. These results also apply to the dual state feedback (SF) case with actuation delays; both produce IFP connections, as shown in Fig. 7.

An additional model to consider from standard controls is output feedback (OF). Consider a system described by

$$\begin{aligned} x_r(t+1) &= A_r x_r(t) + B_{2r} u_r(t) + B_{1r} w(t) \\ y_r(t) &= C_r x_r(t) \end{aligned} \quad (4)$$

where $x_r \in \mathbb{R}^n$, $u_r \in \mathbb{R}^m$, and $y_r \in \mathbb{R}^p$ correspond to states, control action, and sensed outputs, respectively. The OF controller for this system inherently contains IFPs irrespective of delays being present; these are represented by ‘IFP-Sense-2’, ‘IFP-State’, and ‘IFP-Act-2’ in Fig. 2. We shall refer to these as OF-IFPs. IFP-State estimates state evolution in the absence of noise and actuation, IFP-Act-2 accounts for controller action, and IFP-Sense-2 predicts incoming sensory information based on the internal estimated state. We remark that in principle, if only Bayesian estimation of the initial condition is required, no IFPs are required. However, if timely state estimations are required for action (e.g. in the Kalman filter), then OF-style IFP is necessary; thus, IFPs in OF are somewhat Bayesian in nature, they represent more than just pure Bayesian estimation. Additionally, in the adversarial \mathcal{H}_∞ setting, an additional IFP path is necessary to anticipate the worst-case adversarial disturbance.

As with the FC and SF cases, we can introduce internal delay states to introduce sensing and actuation delay. Let the augmented state be $x = [x_r^\top \ x_a^\top \ x_s^\top]^\top$, where x_a represents delayed actuation states and x_s represents delayed sensing states. Then, x_a has length $d_a m$ where d_a is the number of actuation delay steps; the last m elements of x_a represent delayed physical actuation upon the real physical

state x_r . Similarly, x_s has length $d_s p$ where d_s is the number of sensing delay steps; the last p elements of x_s represent delayed information from the sensor. For ease of notation, we assume that $d_a = d_s = d$; our setup trivially extends to the case that they are unequal.

We also augment the input, i.e. $u = [u_r^\top \ u_s^\top]^\top$. Now, u_r represents control input which is will be delayed before reaching the physical states; $u_s \in \mathbb{R}^{pd}$ represent the internal wires to internal delay states x_s (as in the FC case).

Let $Z^{x,y} \in \mathbb{R}^{xy \times xy}$ be the block-downshift matrix, with identity matrices of size y along its first block sub-diagonal and zeros elsewhere. The system matrices for the augmented system are written in block matrix form:

$$\begin{aligned} A &= \begin{bmatrix} A_r & \hat{B}_{2r} & 0 \\ 0 & Z^{d,m} & 0 \\ \hat{C}_r & 0 & Z^{d,p} \end{bmatrix}, B_2 = \begin{bmatrix} 0 & 0 \\ \hat{I}_B & 0 \\ 0 & I \end{bmatrix}, B_1 = \begin{bmatrix} B_{1r} \\ 0 \\ 0 \end{bmatrix} \\ C &= [0 \ 0 \ \hat{I}_C], \text{ where} \\ \hat{B}_{2r} &= [0_{n \times m(d-1)} \ B_{2r}], \hat{C}_r = [C_r^\top \ 0_{n \times p(d-1)}]^\top \\ \hat{I}_C &= [0_{p \times p(d-1)} \ I_{p \times p}], \hat{I}_B = [I_{m \times m} \ 0_{m \times m(d-1)}]^\top \end{aligned} \quad (5)$$

We solve DAREs to obtain the optimal estimator gain $L = [L_1^\top \ L_2^\top \ L_3^\top]^\top$ and optimal controller gain $K = [K_1 \ K_2 \ K_3]$. By virtue of the block-matrix structure of our system matrices, L_2 and K_3 are generally zero. This allows us to simplify the resulting OF estimator and controller into the one shown in Fig. 2. For illustrative purposes, we write the simplified equations for $d = 1$ below, though our observations extend to larger values of d :

$$\begin{aligned} \delta(t+1) &= C_r x_r(t) - C_r \hat{x}_r(t) - L_3 \delta(t) \\ \hat{x}_r(t+1) &= A_r \hat{x}_r(t) + B_{2r} x_a(t) + L_1 \delta(t) \\ u_a(t) &= K_1 \hat{x}_r(t) + K_2 x_a(t) \end{aligned} \quad (6)$$

In Fig. 2, the OF-IFPs, which were present before we introduced delay, are contained within this controller. Additionally, two new sources of IFPs (‘IFP-Sense-1’ and ‘IFP-Act-1’) have been introduced due to delay. These resemble the IFPs from our FC- and SF-only delay models from Fig. 7, respectively. Thus, a kind of separation principle is at play: the total controller is nearly exactly the sum of its parts (FC-delayed, SF-delayed, and OF without delay).

We also note that the delay-motivated IFPs are much bigger in dimension than the OF-IFPs; both have dimension determined by the magnitude of delay (i.e. number of steps) multiplied by number of physical states. Of the three OF-IFPs, IFP-State and IFP-Sense-2 have dimension equal to the number of physical states, while IFP-Act-1 has dimension equal to the number of physical actuators. Together, these five IFPs comprise the main sources of IFP that can be modelled using standard control; all are smaller in dimension and less complex than SLS-based IFP, which is described in our companion paper [2].

V. DISCUSSION

The results of this paper show that dramatic DESS in systems with diverse sensing and actuation can exist, where two poorly performing components separately create a well-functioning system when combined. The results also show the importance of IFPs within delayed components, where the system performance becomes unstable without the correct feedback information. These theoretical considerations can be applied to biological control and to other complex structures that carry out large computations. The natural next steps are to extend the IFP analysis further using SLS (as is done [2]), and to apply this analysis toward real biological architectures via experimentation (as proposed in [1]).

REFERENCES

- [1] A. A. Sarma, J. S. Li, J. Stenberg, G. Card, E. S. Heckscher, N. Kasthuri, T. Sejnowski, and J. C. Doyle, “Internal feedback in biological control: Architectures and examples,” 2021. [Online]. Available: <https://arxiv.org/abs/2110.05029>
- [2] J. S. Li, “Internal feedback in biological control: Locality and system level synthesis,” 2021. [Online]. Available: <https://arxiv.org/abs/2109.11757>
- [3] D. J. Felleman and D. C. V. Essen, “Distributed hierarchical processing in the primate cerebral cortex,” *Cereb Cortex*, pp. 1–47, 1991.
- [4] P. Sterling and S. B. Laughlin, *Principles of neural design*. MIT Press, 2015.
- [5] E. M. Callaway, “Feedforward, feedback and inhibitory connections in primate visual cortex,” *Neural Networks*, vol. 17, no. 5-6, pp. 625–632, 2004.
- [6] L. Muckli and L. S. Petro, “Network interactions: non-geniculate input to V1,” *Current Opinion in Neurobiology*, vol. 23, no. 2, pp. 195–201, 2013.
- [7] N. Suga, “Role of corticofugal feedback in hearing,” *Journal of Comparative Physiology A: Neuroethology, Sensory, Neural, and Behavioral Physiology*, vol. 194, no. 2, pp. 169–183, 2008.
- [8] D. Busse, M. de la Rosa, K. Hobiger, K. Thurley, M. Flossdorf, A. Scheffold, and T. Hofer, “Competing feedback loops shape IL-2 signaling between helper and regulatory T lymphocytes in cellular microenvironments,” *Proceedings of the National Academy of Sciences*, vol. 107, no. 7, p. 3058–3063, Jan 2010.
- [9] J. M. Lund, L. Hsing, T. T. Pham, and A. Y. Rudensky, “Coordination of early protective immunity to viral infection by regulatory T cells,” *Science*, vol. 320, no. 5880, pp. 1220–1224, May 2008.
- [10] N. W. Palm and R. Medzhitov, “Not so fast: adaptive suppression of innate immunity,” *Nature Medicine*, vol. 13, no. 10, pp. 1142–1144, Oct 2007.
- [11] Y. Nakahira, Q. Liu, T. J. Sejnowski, and J. C. Doyle, “Diversity-enabled sweet spots in layered architectures and speed-accuracy trade-offs in sensorimotor control,” *Proceedings of the National Academy of Sciences of the United States of America*, vol. 118, no. 22, pp. 1–11, 2021.
- [12] J. Anderson, J. C. Doyle, S. H. Low, and N. Matni, “System level synthesis,” *Annual Reviews in Control*, vol. 47, pp. 364–393, 2019.
- [13] Y. Nakahira, Q. Liu, T. J. Sejnowski, and J. C. Doyle, “Fitts’ law for speed-accuracy trade-off describes a diversity-enabled sweet spot in sensorimotor control,” *arXiv*, 2019. [Online]. Available: <http://arxiv.org/abs/1906.00905>
- [14] S. Musall, M. T. Kaufman, A. L. Juavinett, S. Gluf, and A. K. Churchland, “Single-trial neural dynamics are dominated by richly varied movements,” *Nature Neuroscience*, vol. 22, no. 10, pp. 1677–1686, 2019.